CHAPTER-II

Photoemission calculation with free electron wavefunction

2.1 Introduction

Photoemission experiments on surfaces of solids are basically concerned with the excitation of electrons by the incident photon energy. A simple calculation of photocurrent (in one electron approximation) involves the evaluation of matrix elements (equation 1.1) of the form $\langle \psi_f | H' | \psi_i \rangle$, where $| \psi_i \rangle$ and $| \psi_f \rangle$ denote the initial and final one-electron states whose energies are connected by $E_f - E_i = \hbar\omega$ and $H' = (e/2mc).(\vec{p}.\vec{A} + \vec{A}.\vec{p})$. $\vec{p}$ being the one-electron momentum operator and $\vec{A}$, the vector potential associated with the photon field. The states $| \psi_i \rangle$ and $| \psi_f \rangle$ are modified from the bulk states by the presence of the surface. Similarly, the photon field also has a spatial variation in the surface region.

In standard photoemission calculations[27,28] the one-electron states are calculated with a high degree of accuracy - but the variation of the photon field is generally neglected. Depending on the type of the experimental data one intends to compare the calculation with, this may or may not be a reasonable approximation. In the case where one looks at the photoemission current as a function of photon energy with a constant initial state, the photon field variation in the surface region needs to be considered more carefully. However, a first principles calculation of the electromagnetic field in the presence of the surface is an extremely complex problem - only for the case of jellium the results are available[19,26]. Bagchi and Kar[33], on the other hand, computed the field in a simple 'local' model, using experimentally determined frequency-dependent dielectric functions as parameter, and they used this for calculation of photocurrent from the surface state of tungsten. This simple model is applicable to those elements for which the frequency-dependent dielectric functions are known. In this chapter, we use this model in conjunction with free-electron wavefunctions for

electron states and show that the results obtained agree qualitatively with experimental data and the theoretical results obtained by more sophisticated jellium field calculations. This would indicate that we may use the simple model for calculation of photoemission cross-section of other metals for which the jellium results would not be applicable. The contents of this chapter have already been published[38]. Subsequently, a successful application in the case of berryllium has also been made[39].

We are considering the photoemission to take place along z-axis, which is normal to the surface. We may therefore write H' as

$$H' = \frac{e\hbar}{imc}\left[\tilde{A}_\omega(z)\frac{d}{dz}+\frac{1}{2}\frac{d}{dz}\tilde{A}_\omega(z)\right]$$

$$\text{where,}\quad \tilde{A}_\omega(z)=\frac{A_\omega(z)}{A_0}$$

with $A_\omega(z)$ as the component of the vector potential along z-axis, and A_0 is the amplitude of the incident beam. The formula for photoemission cross-section (equation 1.1) can be written as

$$\frac{d\sigma}{d\Omega} \approx \frac{k_f^2}{\omega}\left|\langle\psi_f|\tilde{A}_\omega(z)\frac{d}{dz}+\frac{1}{2}\frac{d}{dz}\tilde{A}_\omega(z)|\psi_i\rangle\right|^2$$

(2.1)

To evaluate the matrix element in equation (2.1) we have to construct ψ_i, ψ_f and determine $\vec{A}_\omega$.

2.2 Initial and final state wavefunctions

The wavefunctions for both the initial and final states are calculated in the free electron model with the potential given by

$$V(z)=V_0\theta(z) \qquad \text{where,}\quad V_0=E_F+\phi$$

E_F being the energy at the Fermi level in the free electron model and ϕ the work function, $\theta(z)$ is the step function defined as: $\theta(z)=0$ for $z<0$

and $\theta(z)=1$ for $z>0$ as shown in fig 2.1. By matching the wavefunctions at the surface plane $z=0$, we may write the initial state wavefunction as

$$\psi_i(\vec{r}) = \begin{cases} \left[e^{ik_i z} + \dfrac{ik_i+\chi}{ik_i-\chi} e^{-ik_i z}\right] e^{i\vec{k}_\parallel \cdot \vec{r}_\parallel} & z<0 \\ \dfrac{2ik_i}{ik_i-\chi} e^{-\chi z} e^{i\vec{k}_\parallel \cdot \vec{r}_\parallel} & z>0 \end{cases}$$

$$\text{where,} \quad k_i^2 = \frac{2m}{\hbar^2} E_i - \vec{k}_\parallel^2, \quad \chi^2 = \frac{2m}{\hbar^2}(V_0 - E_i) + \vec{k}_\parallel^2$$

(2.2)

and $\vec{k}_\parallel$ and $\vec{r}_\parallel$ are the components of $\vec{k}$ and $\vec{r}$ in the x-y plane i.e. the plane parallel to the surface.

Similarly, the final state wavefunction may be written as

$$\psi_f(\vec{r}) = \begin{cases} \left[e^{iqz} + \dfrac{q-k_f}{q+k_f} e^{-iqz}\right] e^{i\vec{k}_\parallel \cdot \vec{r}_\parallel} & z>0 \\ \dfrac{2q}{q+k_f} e^{ik_f z} e^{i\vec{k}_\parallel \cdot \vec{r}_\parallel} & z<0 \end{cases}$$

$$\text{where,} \quad \vec{k}_f^{\,2} = \frac{2mE_f}{\hbar^2} - \vec{k}_\parallel^2, \quad \vec{q}^2 = \frac{2m}{\hbar^2}(E_f - V_0) - \vec{k}_\parallel^2, \quad E_f = E_i + \hbar\omega$$

(2.3)

2.3 Photon field

The model of Bagchi and Kar[33] is employed for the computation of $A_0(z)$. We assume the z-direction to be perpendicular to the nominal surface which is chosen as $z=0$. The slight change made from the model of Bagchi & Kar seems to be more realistic to us and is also more convenient when we want to include the periodic potential later. The metal is assumed to occupy all space to the left of the $z=0$ plane as shown in fig 2.2. The response of the electromagnetic field is bulk-like

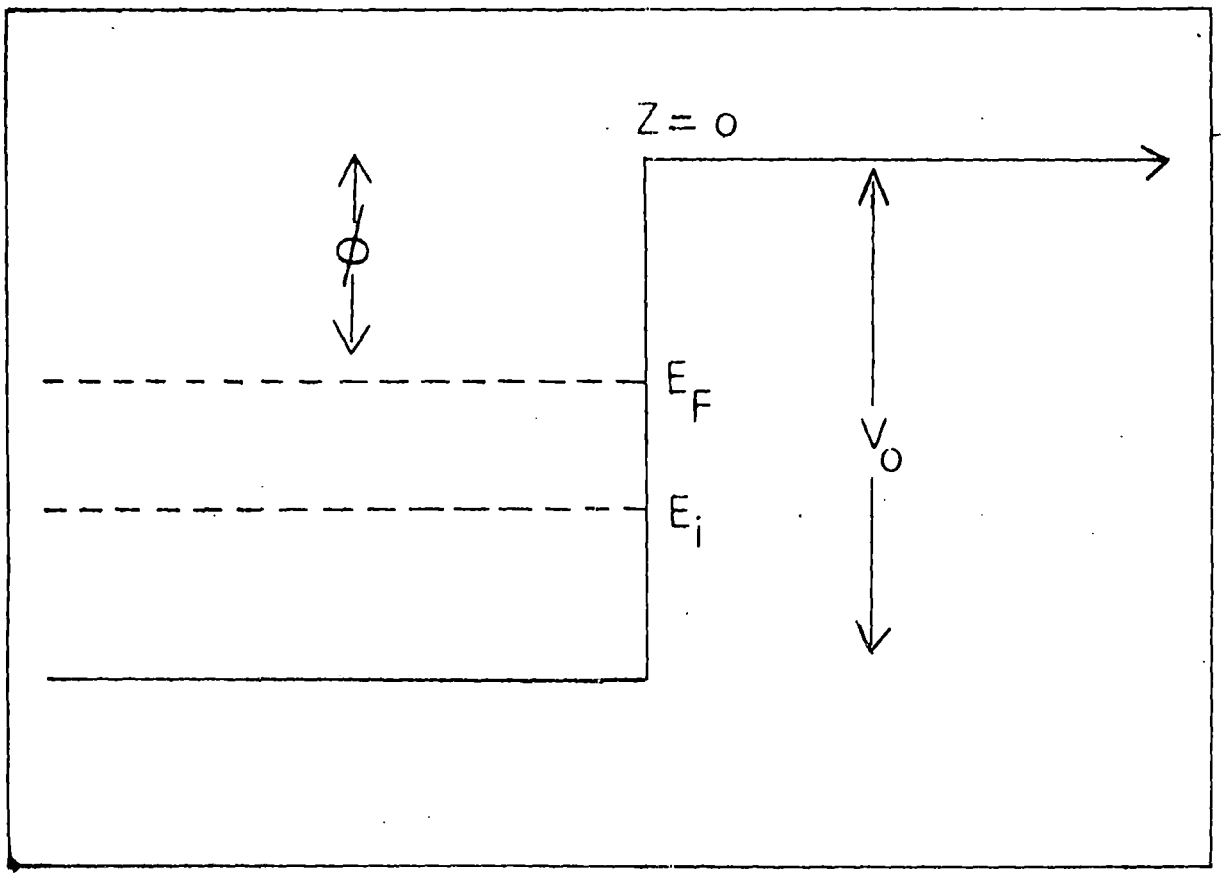

Fig 2.1 Model potential used for calculating wavefunctions for initial and final states. ϕ=4.25 eV & V_o=15.95 eV

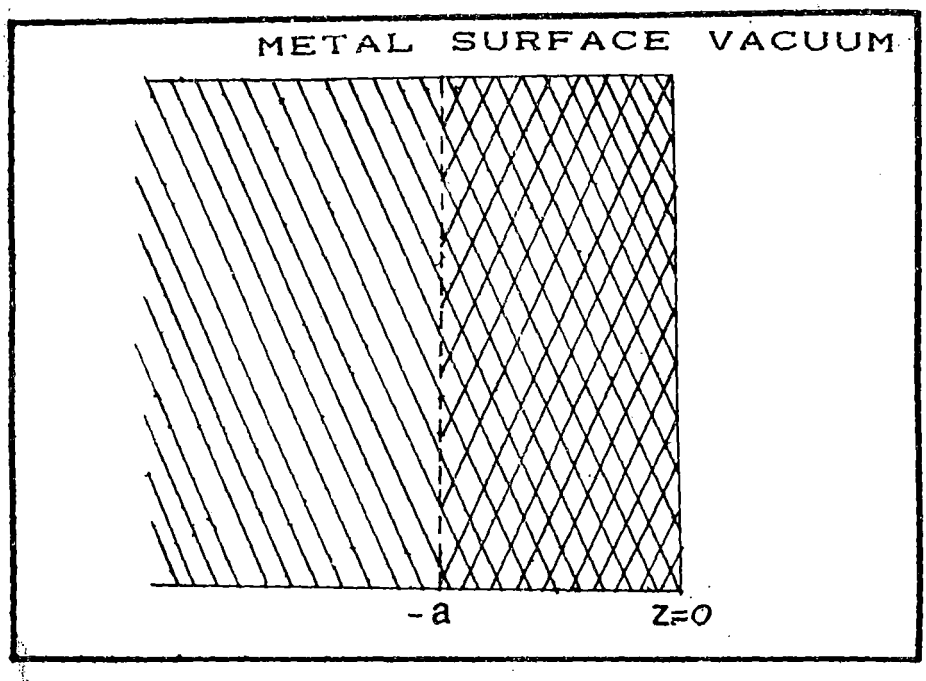

Fig 2.2 Schematic representation of the surface region used in the model

everywhere except in the surface region defined by $-a \leq z \leq 0$. In this region the model dielectric function is chosen to be a local one which interpolates linearly between the bulk value inside the metal and the vacuum value (unity) outside. The model frequency-dependent dielectric function is therefore given by

$$\epsilon(\omega) \equiv \begin{cases} \epsilon_1(\omega) + i\epsilon_2(\omega) & z < -a \\ 1 + [1-\epsilon(\omega)]\frac{z}{a} & -a \leq z \leq 0 \\ 1 & z > 0 \end{cases}$$

For the complex dielectric function $\epsilon(\omega,z)$ we use the experimental values given by Weaver[35]. We consider p-polarised light to be incident on the surface plane making an angle θ_i with the z-axis. We have chosen the origin to be at the metal-vacuum interface instead of at the centre of the surface region and by substituting (z+a/2) for z in equation (1.3) the calculated vector potential of interest, $A_\omega(z)$, in the long-wavelength limit $(\omega a/c) \to 0$ is

$$\tilde{A}_\omega(z) = \begin{cases} -\dfrac{\sin 2\theta_i}{\sqrt{[\epsilon(\omega) - \sin^2\theta_i]} + \epsilon(\omega)\cos\theta_i} & z < -a \\ -\dfrac{\sin 2\theta_i}{\sqrt{[\epsilon(\omega) - \sin^2\theta_i]} + \epsilon(\omega)\cos\theta_i} \dfrac{a\epsilon(\omega)}{[1-\epsilon(\omega)]z + a} & -a \leq z \leq 0 \\ -\dfrac{\epsilon(\omega)\sin 2\theta_i}{\sqrt{[\epsilon(\omega) - \sin^2\theta_i]} + \epsilon(\omega)\cos\theta_i} & z > 0 \end{cases}$$

(2.4)

2.4 Cross-section calculation

To calculate the photoemission cross-section we have to integrate the matrix element in equation (2.1) over the different regions of the solid i.e., vacuum, surface and bulk region using the expressions for Ψ_i,

ψ_f and $\vec{A}_\omega$ (equations 2.2-4) as

$$I = \int_{-\infty}^{\infty} \psi_f^* \left[\tilde{A}_\omega(z) \frac{d}{dz} + \frac{1}{2} \left[\frac{d}{dz} \tilde{A}_\omega(z) \right] \right] \psi_i dz$$

$$= \int_{-\infty}^{-a} \psi_f^* \tilde{A}_\omega(z) \frac{d\psi_i}{dz} dz + \int_{-a}^{0} \psi_f^* \tilde{A}_\omega(z) \frac{d\psi_i}{dz} dz$$

$$+ \frac{1}{2} \int_{-a}^{0} \psi_f^* \left[\frac{d}{dz} \tilde{A}_\omega(z) \right] \psi_i dz + \int_{0}^{\infty} \psi_f^* \tilde{A}_\omega(z) \frac{d\psi_i}{dz} dz$$

(2.5)

In the following sections we shall calculate each of the integral in equation (2.5) over the different region of the solid :

a) Bulk region

The photon field equation (2.4) is a constant here and we calculate analytically the first term of equation (2.5) as

$$I_1 = \int_{-\infty}^{-a} \psi_f \tilde{A}_\omega(z) \frac{d\psi_i}{dz} dz$$

$$= \frac{2qA_1}{q+k_f} \int_{-\infty}^{-a} e^{-ik_f z} e^{\alpha z} ik_i \left[e^{ik_i z} - \frac{ik_i+\chi}{ik_i-\chi} e^{-ik_i z} \right] dz$$

$$= iC_1 k_i \left[\frac{e^{-\alpha a} e^{-i(k_i-k_f)a}}{\alpha+ik_i-ik_f} - \frac{ik_i+\chi}{ik_i-\chi} \frac{e^{-\alpha a} e^{i(k_i+k_f)a}}{\alpha-ik_i-ik_f} \right]$$

where, $C_1 = \frac{2qA_1}{q+k_f}$ and $A_1 = -\frac{\sin 2\theta_i}{\sqrt{[\epsilon(\omega)-\sin^2\theta_i]+\epsilon(\omega)\cos\theta_i}}$

(2.6)

b) Surface region

It is already mentioned that the extent of the surface region is $-a \le z \le 0$ and the photon field has a spatial variation over this region and we calculate numerically two terms (2nd & 3rd term of equation 2.5) as

$$I_2 = \int_{-a}^{0} \psi_f \tilde{A}_\omega(z) \frac{d\psi_i}{dz} dz$$

$$= ik_i C_2 \int_{-a}^{0} \frac{e^{-ik_f z}}{\frac{z}{a} + B_1} \left[e^{ik_i z} - \frac{ik_i + \chi}{ik_i - \chi} e^{-ik_i z} \right] e^{\alpha z} dz$$

and $$I_3 = \frac{1}{2} \int_{-a}^{0} \psi_f^* \frac{d\tilde{A}_\omega}{dz} \psi_i dz$$

$$= -\frac{1}{2a} C_2 \int_{-a}^{0} \frac{e^{-ik_f z}}{\left(\frac{z}{a} + B_1\right)^2} \left[e^{ik_i z} + \frac{ik_i + \chi}{ik_i - \chi} e^{-ik_i z} \right] e^{\alpha z} dz$$

where, $B_1 = \frac{1}{1 - \epsilon(\omega)}$ and $C_2 = C_1 B_1 \epsilon(\omega)$

(2.7)

c) Vacuum region

Photon field has no spatial variation in the vacuum region and we calculate the 4th term of equation (2.5)

$$I_4 = \int_{0}^{\infty} \psi_f \tilde{A}_\omega(z) \frac{d\psi_i}{dz} dz$$

$$= ik_i C_3 \int_{0}^{\infty} \left[e^{-iqz} + \frac{q - k_f}{q + k_f} e^{iqz} \right] e^{-\chi z} dz$$

$$= ik_i C_3 \left[\frac{1}{iq + \chi} + \frac{q - k_f}{q + k_f} \frac{1}{\chi - iq} \right]$$

where, $C_3 = \frac{2A_1(-\chi)\epsilon(\omega)}{ik_i - \chi}$

(2.8)

The general expression for photoemission (equation 2.1) in terms of I_1, I_2, I_3 and I_4 would be

$$\frac{d\sigma}{d\omega} \approx \frac{k_f^2}{\omega} |I_1+I_2+I_3+I_4|^2$$

(2.9)

Using equations (2.6-2.9) we have calculated photocurrent numerically. Some portions of the computer programs are given in the appendix-II. However, to ensure convergence for z<0, one has to introduce a convergence factor due to lifetime effects. This is a standard procedure in Low Energy Electron Diffraction and photoemission calculations (see, for example, Pendry[36]). We do it here by introducing a factor $e^{-\alpha z}$ (for z<0) in the calculation of the matrix element - this is to take into account the inelastic scattering of electrons.

2.5 Results and discussion

We have applied our results for computing the normal photoemission from the Fermi level of aluminium (100) face, for which the experimental results as well as theoretical calculations using jellium model are available. The experimental results are shown in fig 2.3, the data of Levinson *et al*[20] having been used. For our calculations[38], we have taken ϕ = 4.25 eV and E_F=11.7 eV - these values have been given by Ashcroft and Mermin[37]. Since normal photoemission is considered $\vec{k}_{\parallel}$ =0; also θ_i is taken to be 45^0 as in the experiment. Our results for the photoemission cross-section are shown in fig 2.4 (with a= 10 atomic units). We see that there is qualitative agreement between the experimental data and the calculated photo-current. The calculated curve shows a peak at 11 eV, a minimum at 15 eV (~ plasmon energy) and again a broad peak around 20.5 eV. These features are also present in the experimental curve - although the ratio of the peak heights of the two peaks (below and above the plasmon energy) in the calculated and

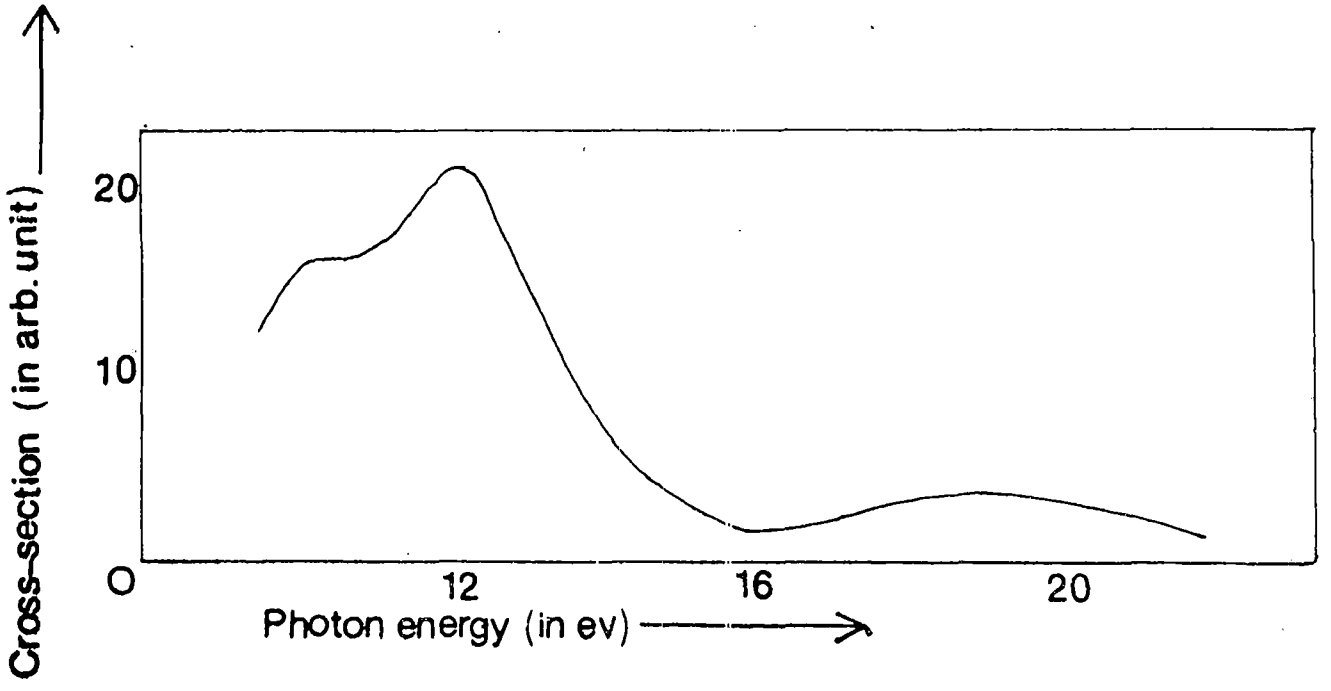

Fig 2.3 Experimental data of photoemission cross-section (in arb. unit) for normal photoemission from Fermi level aluminium (100) as a function of photon energy

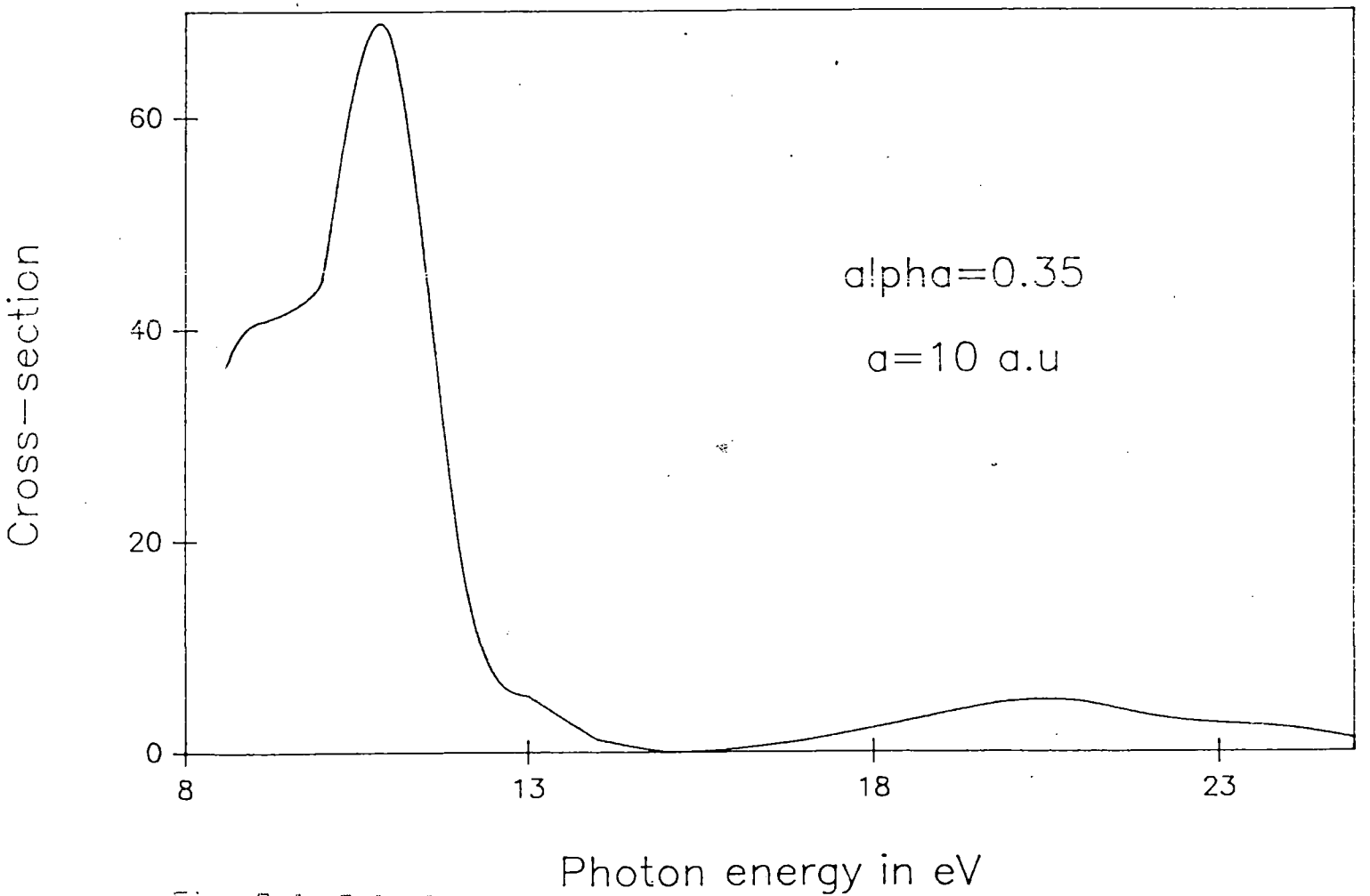

Fig 2.4 Calculated photoemission cross-section (in arb unit) for normal photoemission from Fermi level of aluminium (100) as a function of photon energy

experimental curve is different.

We further investigated the origin of the peak at 11 eV in the calculated spectrum and concluded that it is a surface feature. As evidence for that we plot the field $|A_\omega(z)|$ as a function of z in the surface region for $\hbar\omega$=11 eV (fig 2.5). We see that there is strong peak in the middle of the surface region. For $\hbar\omega$=15 eV and 20 eV, on the other hand, the plot of $|A_\omega(z)|$ does not show any peak in the surface region.

As further evidence of the peak at 11 eV being surface related, we show the results of a calculation of photo-current with fields given by the Fresnel refraction formula (obtained by putting a=0 in equation 2.4)

$$\tilde{A}_\omega(z) = \begin{cases} -\dfrac{\sin 2\theta_i}{\sqrt{[\epsilon(\omega)-\sin^2\theta_i]}+\epsilon(\omega)\cos\theta} & z<0 \\ -\dfrac{\epsilon(\omega)\sin 2\theta_i}{\sqrt{[\epsilon(\omega)-\sin^2\theta_i]}+\epsilon(\omega)\cos\theta} & z>0 \end{cases}$$

and the (free-electron) wavefunctions are the same as in equations (2.2-3). We see that, although there is a minimum around 12 eV, there is no peak around 11-12 eV (fig 2.6). Above the plasmon frequency, the curve shows a peak which is much more pronounced than that in the calculation with a surface region (fig 2.4). The peak in the experimental data above the plasmon frequency is also much less pronounced. Anyway, it is quite clear that the calculations with the simple Fresnel refraction formula is not even qualitatively correct - in particular, it completely fails to reproduce the peak around 11-12 eV.

We have thus shown that with a simple local model for the dielectric function, we can get a qualitative agreement with experimental data. There have been previous calculations, notably by

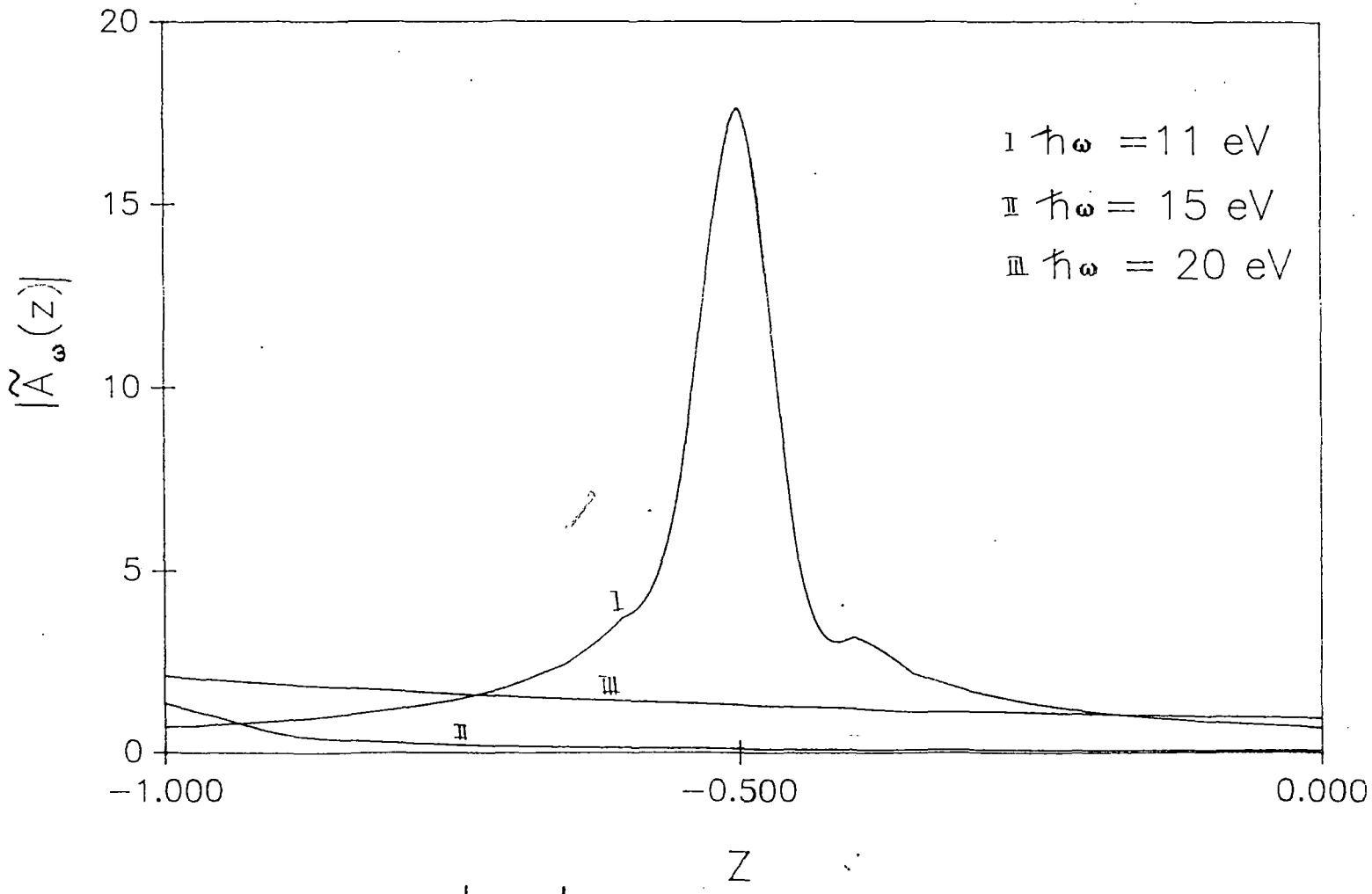

Fig 2.5 Plot of $|A\omega(z)|$ versus z in the surface for $\hbar\omega$ =11 eV, 15 eV and 20 eV for aluminium

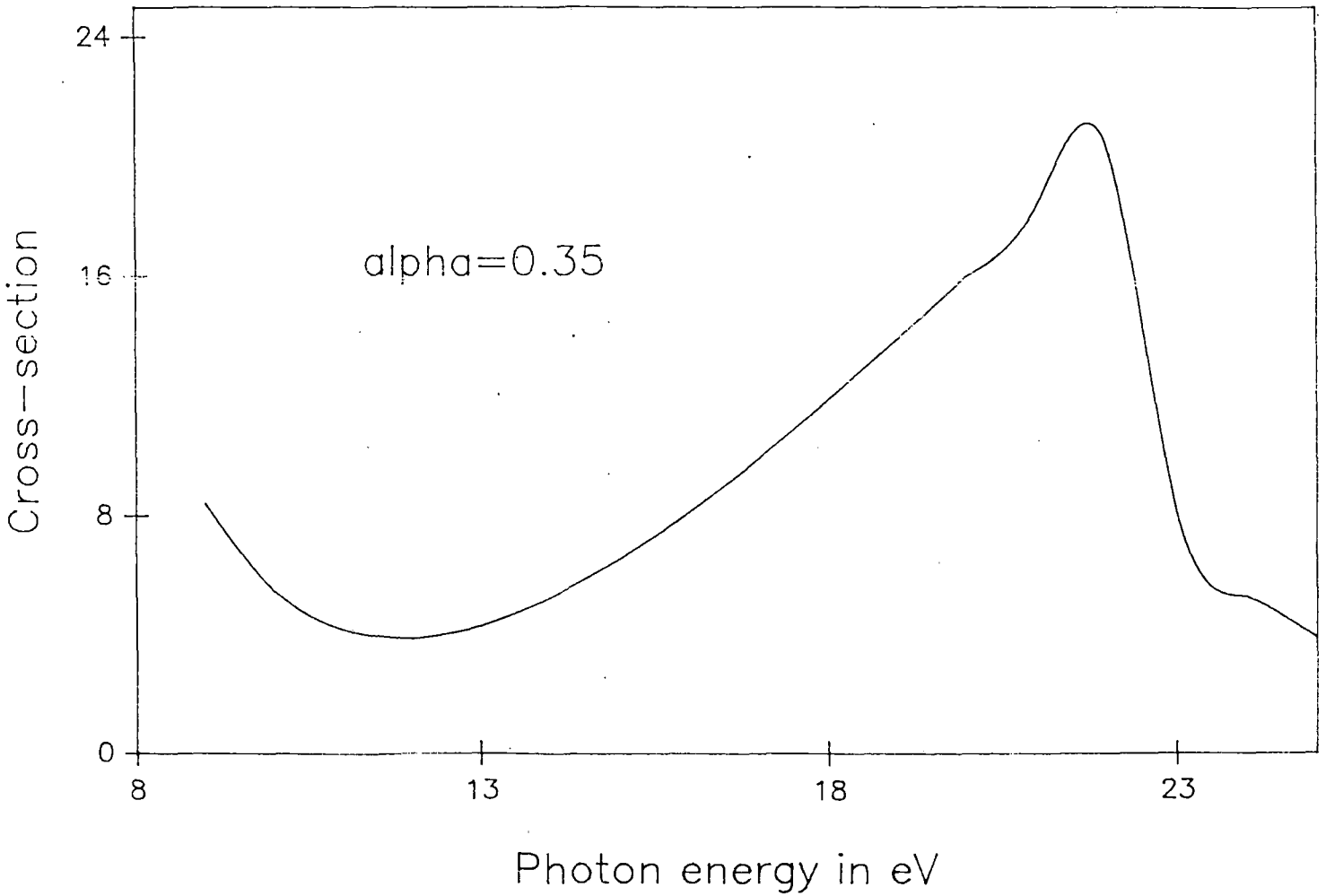

Fig 2.6 Photoemission cross-section (in arb. unit) for normal emission from Fermi level of aluminium with Fresnel fields

Levinson et al[20] and Barberan and Inglesfield[22] for aluminium. Kempa and others[21] have also considered the photoyield in terms of the hydrodynamical model and attributed the 12 ev peak to plasma waves. The calculations of Levinson et al, employing the self-consistent jellium model for fields in the surface region are more sophisticated and their results are in better agreement with the experimental data. However, the calculations for jellium can not be extended to more complicated cases, e.g., transition metals and semiconductors, while the model we have employed can be extended to these cases. So the qualitative agreement we obtain in aluminium and the previous application of the same model to the case of tungsten[33] gives us confidence to apply our model to photoemission calculations for other metals and semiconductors. However, for these cases, we can not use free electron wavefunctions any more.

In conclusion, although there are shortcomings in the model for electromagnetic field employed here (for example, since experimentally measured dielectric functions are used as inputs, the physical origin of the surface- related peak cannot be pin-pointed) -it gives results in reasonable agreement with experimental data, and has the potential of being used for a number of metals and semiconductors. In the next chapter, we shall combine a better description of the wavefunction with the field given by this model for photo-current calculations.